

The Pixon Method of Image Reconstruction

Richard C. Puetter

*Center for Astrophysics and Space Sciences, University of California,
San Diego, La Jolla, CA 92093-0424, USA*

Amos Yahil

*Department of Physics and Astronomy, State University of New York,
Stony Brook, NY 11794-3800, USA*

Abstract. The Pixon method is a high-performance, nonlinear image reconstruction method that provides statistically unbiased photometry and robust rejection of spurious sources. Relative to other methods, it can increase linear spatial resolution by a factor of a few and sensitivity by an order of magnitude or more. All of these benefits are achieved in computation times that can be orders of magnitude faster than its best competitors.

1. Introduction

Optimal extraction of the underlying quantities from measured data requires the removal of measurement defects such as noise and limited instrumental resolution. When the underlying quantity is an image, this process is known as image reconstruction (sometimes called image restoration, if the data are also in the form of an image).

The original Pixon method (Piña & Puetter 1993; Puetter & Piña 1993; Puetter 1995, 1997) was developed to eliminate problems with existing image reconstruction techniques, particularly signal-correlated residuals and the production of spurious sources. This was followed by the accelerated Pixon method that vastly increased the computational speed (Yahil & Puetter, in preparation). Recently, a quick Pixon method was developed that is even faster, at the expense of some photometric inaccuracy for low signal-to-noise-ratio features (Puetter & Yahil, in preparation). Nevertheless, the quick Pixon method provides excellent results for a wide range of imagery and, with special-purpose hardware now under design, is capable of real-time video image reconstruction.

Since its inception, the Pixon method in its various forms has been applied to a wide variety of astronomical, surveillance, and medical image reconstructions (spanning all wavelengths from γ -rays to radio), as well as to spectroscopic data. In all cases tested so far, both by the authors and by a variety of other workers, the Pixon method has proved superior in quality to all other methods and computationally much faster than its best competitors.

A patent for the Pixon method is pending, restricting its commercial use. For individual scientific purposes, the original Pixon method is freely available

in IDL and C++ from the San Diego Supercomputer Center¹. The accelerated and quick Pixon methods are sold by our company, Pixon LLC, but special arrangements for their free use in selected scientific projects can be made.

The next sections discuss image reconstruction in general (§2.), describe the Pixon method (§3.), and give some examples (§4.). The HTML and PDF versions of this paper contain numerous additional examples via clickable hyperlinks. The complete set of public image reconstructions, including videos, can be seen on our Web site².

2. Image Reconstruction Methods

For data taken with linear detectors, image reconstruction often becomes a matter of inverting an integral relation of the form

$$D(\mathbf{x}) = \int d\mathbf{y} H(\mathbf{x}, \mathbf{y}) I(\mathbf{y}) + N(\mathbf{x}) \quad . \quad (1)$$

Here D are the data, I is the sought underlying image model, H is the point-spread function (PSF) due to instrumental and possibly atmospheric blurring, and N is the noise. To avoid confusion, we use the term image to refer exclusively to the true underlying image or its model. Contrary to common parlance, the data are never called the image. We clearly distinguish between abstract image space and real data space, with the PSF transforming from the former to the latter.

If the PSF is only a function of the displacement, $H(\mathbf{x}, \mathbf{y}) = H(\mathbf{x} - \mathbf{y})$, then the integral in equation (1) becomes a convolution, but in general the PSF can vary across the field. Note that the data need not have the same resolution as the image, or even the same dimensionality. For example, the Infrared Astronomical Satellite (IRAS) provided 1-D scans across the 2-D sky, and tomography data consist of multiple 2-D projections of 3-D images. Another common case is of data consisting of multiple, dithered, exposures of the same field, which all need to be modeled by a single image, possibly with PSFs that vary from one exposure to another.

Image reconstruction differs from standard solutions of integral equations due to the noise term, N , whose nature is only known statistically. Methods for solving such an equation fall under two broad categories. (1) Direct methods apply explicit operators to the data to provide estimates of the image. These methods are often linear, or have very simple nonlinear components. Their advantage is speed, but they typically amplify noise, particularly at high frequencies. (2) By contrast, indirect methods model the noiseless image, transform it only forward to provide a noise-free data model, and fit the parameters of the image to minimize the residuals between the real data and the noise-free data model. The advantage of indirect methods is that noise is supposedly excluded (but see §2.3.). Their disadvantage is the required modeling of the image. If a good parametric form for the image is known a priori, the result can be superb.

¹<http://pixon.sdsc.edu>

²<http://www.pixon.com>

If not, either the derived image badly fits the data or, conversely, it overfits the data, interpreting noise as real features. Indirect methods are typically significantly nonlinear and much slower than direct methods.

The Pixon method is a nonparametric, indirect, reconstruction method. It avoids the pitfalls of other indirect methods, while achieving a computational speed on a par with direct methods. To appreciate its advantages we therefore first provide a brief description of some competing direct and indirect methods.

2.1. Direct Methods

In the case of a position-independent PSF, naive image deconvolution is obtained by inverting the integral equation (1) in Fourier space, ignoring the noise:

$$\tilde{I}(\mathbf{k}) = \tilde{D}(\mathbf{k})/\tilde{H}(\mathbf{k}) \quad , \quad (2)$$

where the tilde designates Fourier transform, and \mathbf{k} is the spatial wavenumber. This method amplifies noise at high frequencies, since $H(\mathbf{k})$ is a rapidly declining function of $|\mathbf{k}|$, while $D(\mathbf{k})$, which includes high-frequency noise, is not.

To minimize noise amplification, nonlinear filtering is often applied to the data prior to Fourier inversion. Common filters are those due to Wiener (1949) (see also Press et al. 1992) and thresholding of wavelet transforms (e.g., Donoho & Johnstone 1994; Donoho 1995). The Wiener filter has the advantage of being applied in Fourier space. Wavelet thresholding requires a wavelet transform, thresholding, and a back wavelet transform, all followed by Fourier inversion. Demonstrations of the superior performance of the Pixon method relative to Wiener-filtered Fourier inversions can be seen on our Web site in the reconstruction of the Lena image and an aerial view of New York City.

2.2. Parametric Least-Squares Fit

The simplest indirect image reconstruction is a least-squares fit of a parametric model with a small number of parameters compared to the number of data points. Originally due to Gauss, this method is always superior to other methods, provided that the image can be so modeled. It is equivalent to a maximum-likelihood optimization in which the residuals are assumed to be Gaussian distributed. All models within the restricted parameterization are considered equally likely, and the likelihood function maximized is $P(D|I)$, the conditional probability of the data, given the model image. For this reason, the method is also known as maximum a posteriori probability (MAP) image reconstruction.

2.3. Nonnegative Least-Squares Fit

When no parametric model of the image is known, the number of image model parameters can quickly become comparable to, or exceed, the number of data points. In this case, a MAP solution becomes inappropriate. For example, if the number of points in the image model equals the number of data points, then the nonsingular nature of the linear integral transform in equation (1) assures that there is a solution for which the data, including the noise, are exactly modeled with zero residuals. This is clearly the same poor solution, with all its noise amplification, obtained by the naive Fourier deconvolution.

The above example shows that an unrestricted indirect method is no better at controlling noise than a direct method, and therefore the model image must be restricted in some way. The indirect methods described below all restrict the image model and differ only in the specifics of image restriction.

A simple restriction is to constrain the model image to be positive. Since even a delta-function image is broadened by the PSF, it follows that the exact inverse of any noisy data with fluctuations on scales smaller than the PSF must be both positive and negative. By preventing the image from becoming negative, the noise-free data model cannot fluctuate on scales smaller than the PSF, which is equivalent to smoothing the data on the scale of the PSF.

While smoothing over the scale of the PSF helps to reduce noise fitting, it does not go far enough. The Pixon method (§3.) smoothes further where possible, and is therefore able to eliminate noise fitting on larger scales. Demonstrations of its superior performance relative to nonnegative least squares can be seen on our Web site in the reconstruction of γ -ray imaging in the direction of Virgo, as well as in the Lena and New York City reconstructions.

2.4. Maximum-Entropy Method

Bayesian methods go a step further by assigning explicit a priori probabilities to different models and then maximizing the joint probability of the model and the data:

$$P(I \cap D) = P(D|I)P(I) = P(I|D)P(D) \quad . \quad (3)$$

The model probability function, $P(I)$, is known as the prior. For example, the nonnegative least-squares method (§2.3.) is a Bayesian method with all non-negative models assigned equal nonzero probability and all other models zero probability.

The rationale behind Bayesian methods is to optimize $P(I|D)$, the conditional probability of the image given the data. This probability is proportional to the joint probability $P(I \cap D)$, since the data are fixed, and $P(D)$ can be viewed as a constant. However, it is important to recognize that, unlike $P(D|I)$ which depends on the instrumental response function and noise statistics, $P(I|D)$ is not known from first principles. In practice, therefore, computing $P(I \cap D)$ requires the specification of a completely arbitrary prior, $P(I)$.

The maximum-entropy method (MEM) is the most popular Bayesian image reconstruction technique. It uses the prior

$$P(I) = \exp \left(-\alpha \sum_i I_i \ln I_i \right) \quad , \quad (4)$$

where the sum is over the image pixels, and α is an adjustable parameter designed to strike a balance between image smoothness and goodness of fit. (See Gull 1989 and Skilling 1989 for a discussion of a “natural” choice for α .)

The sum in equation (4) approximates the information entropy of Shannon (1948), which is maximized for a homogeneous image. By favoring a flat image, MEM therefore eliminates structure not required by the data and suppresses noise fitting. The fundamental difficulty with this approach is that the MEM prior is a global constraint (specifically, the prior is invariant under random scrambling of the pixels). MEM therefore enforces an average smoothness on

the entire image and does not recognize that the density of information content in the image varies from location to location. Hence, MEM must necessarily oversmooth the image in some regions and undersmooth it in others. More sophisticated MEM schemes try to remedy this situation by applying separate MEM priors in different parts of the image, or by modifying the logarithmic term to $\ln(I_i/M_i e)$, where M is some preassigned model and e is the base of the natural logarithm (Burch, Gull, & Skilling 1983), but there is additional arbitrariness in the choice of M .

By contrast, the Pixon method (§3.) adapts itself to the distribution of information content in the image. Demonstrations of its superior performance relative to MEM are given below (§4.) and on our Web site in a reconstruction of hard X-ray observations of a solar flare.

3. The Pixon Method

Unlike Bayesian methods, the Pixon method (Piña & Puetter 1993; Puetter & Piña 1993; Puetter 1995, 1997) does not assign explicit prior probabilities to image models. Instead, it restricts them by seeking minimum complexity (Solomonoff 1964; Kolmogorov 1965; Chaitin 1966), which not only enables an efficient representation of the image but is also the best way to separate signal from noise.

In simple terms, the Pixon method implements the principle of *Ockham's Razor* to select the simplest plausible model of the image. Clearly, if the signal in the image can be adequately represented by a minimum of P parameters, adding another parameter only serves to introduce artifacts by fitting the noise. Conversely, the removal of a parameter results in an improper representation of the image, since adequate fits to the image require a minimum of P parameters.

While few would dispute that a model with minimum complexity (also called algorithmic information content) is optimal, in practice it is impossible to find such a model for any but the most trivial problems. For example, one might try to model an image as the smallest number of contiguous patches of homogeneous intensity that still adequately fit the data. While there clearly is such a solution, it is quite another matter to find it among the combinatorially large number of possible patch patterns. And we have not even begun to consider patches that are not completely homogeneous.

The Pixon method overcomes this difficulty in the same practical spirit in which other combinatorial problems have been solved, such as the famous traveling salesman problem (e.g., Press et al. 1992). One finds an intelligent scheme in which complexity is reduced significantly in a manageable number of iterations. After that, the decline in complexity per iteration drops sharply, and the process is halted. The solution found in this manner may not have the ultimate minimum complexity, but it is already so superior to other models that it is worth adopting.

The Pixon method minimizes complexity by smoothing the image model *locally* as much as the data allow, thus reducing the number of independent patches, or Pixon elements, in the image. Formally, the image is written as an

integral over a pseudoimage

$$I(\mathbf{y}) = \int \mathbf{dz} K(\mathbf{y}, \mathbf{z}) \phi(\mathbf{z}) \quad , \quad (5)$$

with a positive kernel function, K , designed to provide the smoothing. As in the case of the nonnegative least-squares fit, requiring the pseudoimage, ϕ , to be positive eliminates fluctuations in the image, I , on scales smaller than the width of K . Importantly, this scale is adapted to the data. At each location, it is allowed to increase in size as much as possible without violating the local goodness of fit (GOF). Where the kernel is a delta function, the Pixion element spans one pixel, and the Pixion method reduces to a nonnegative least-squares fit, with the noise-free data model smooth on the scale of the PSF. Where the data allow smoothing on larger scales, however, the Pixion elements become larger. As a result, the overall number of Pixion elements in the image drops, and complexity is reduced.

Complexity can be reduced not only by having kernel functions of different sizes to allow for multi-resolution, but also by a judicious choice of their shapes. For example, circularly symmetric kernels, which might be adequate for the reconstruction of most astronomical images, are not the most efficient smoothing kernels for images with elongated features, e.g., an aerial photograph of a city. Altogether the choice of kernels is the language by which the image model is specified, which should be rich enough to characterize all the independent elements of the image. We have found, in practice, that circular kernels spanning 3–5 octaves in size, with 2–4 kernels per octave, are adequate for most image reconstructions. Additional elliptical kernels are needed only for images with clearly elongated features.

The Pixion reconstruction consists of a simultaneous search for the broadest possible kernel functions and their associated pseudoimage values that together provide an adequate fit to the data. In practice, the details of the search vary depending on the flavor of the Pixion method used. Generally, however, one alternately solves for the pseudoimage given a Pixion map of kernel functions and then attempts to increase the scale sizes of the kernel functions given the current image values. The number of iterations required varies depending on the complexity of the image, but for most problems a couple of iterations suffice.

The essence of the Pixion method is the imposition of the local criteria by which the kernel functions are chosen. For each pixel in pseudoimage space, the combination of the Pixion kernel and the PSF define a footprint in data space. We accept the largest Pixion kernel whose GOF and signal-to-noise ratio (SNR) within that footprint pass predetermined acceptance conditions set by the user. If no kernel has adequate GOF we assign a delta-function kernel, provided that the SNR for its footprint is high enough. If the SNR also fails to meet our condition, no kernel is assigned.

The strength of the Pixion method is in its rejection of features that do not meet strict statistical acceptance criteria. Precisely because of this conservatism, which results in a significant lowering of the noise floor, the Pixion reconstruction is able to find weak but significant features missed by other methods and to resolve all features better. Sensitivity is often improved by an order of magnitude or more relative to competing methods and resolution by a factor of a few.

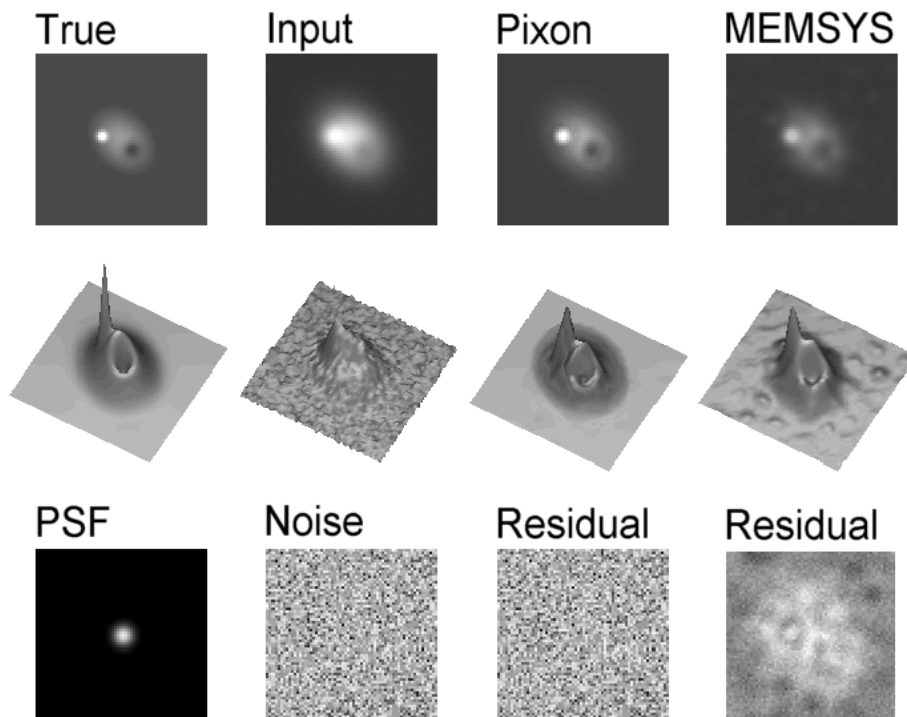


Figure 1. Pixon and MEM restorations, showing PSF (Gaussian, FWHM=6 pixels), true image, Gaussian noise, restored images and residuals. Peak SNR=20; SNR=12 at the bottom of the “hole”. (Reproduced from Puetter 1994.)

Note that the SNR required by the Pixon method is not per pixel in the data, but the overall SNR in the data footprint of the Pixon kernel. The Pixon method is just as powerful in detecting large, low-surface-brightness features as small features with higher surface brightness. Acceptance or rejection of the feature is based in both cases on the *statistical significance* demanded by the user. Demonstrations of the ability of the Pixon method to reconstruct images with low SNR can be seen in the mammogram example (Fig. 3 below) and in the reconstruction of γ -ray imaging in the direction of Virgo on our Web site.

Finally, note that with a very terse representation that only has a small number of nonzero pseudoimage values, the image is also represented in a very compressed form. In the field of data compression one normally distinguishes between strong but lossy versus moderate and non-lossy compression. The Pixon method defines a new type of noiseless compression. The signal is preserved and restorable, while the noise is eliminated. This mode of compression is ideal, since compression can easily reach a factor of 100 for a typical image, yet the only loss is that of unwanted noise. A compressed form of the code is now under design; current codes, however, are primarily built for accuracy and speed and do not yet achieve such high compression.

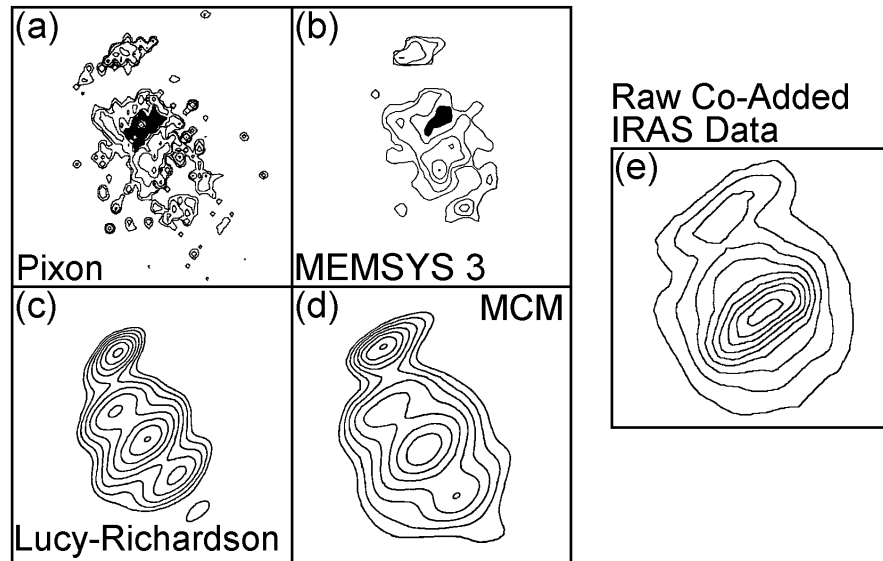


Figure 2. Comparison of reconstruction methods for the interacting galaxy pair M51: (a) Pixion method (Puetter & Piña 1994), (b) Maximum entropy method (Bontekoe et al. 1991), (c) Lucy-Richardson method (Rice 1993), (d) Maximum-Correlation Method, (Rice 1993, used by the HIRES package of NASA's Infrared Processing and Analysis Center), and (e) the raw co-added image.

4. Examples of Pixion Reconstructions

The Pixion method has now been used in a variety of applications by the authors and others (see Puetter 1995, 1997 and references therein). In this section we present a few examples of Pixion reconstructions for a variety of applications. Additional examples can be found in the brochure and figures on our Web site.

4.1. A Synthetic Data Set

The example presented in Fig. 1 (or its color version on our Web site) provides one of the best examples of comparative results of MEM and the Pixion method for a synthetic data set, i.e., a data set with known properties. The MEM algorithm used was MEMSYS 5, the most current release of the MEMSYS algorithms developed by Gull and Skilling (Gull & Skilling 1991). The MEMSYS reconstruction was performed by Nick Weir, and was enhanced by his multichannel correlation method (Weir 1991). As can be seen, the Pixion reconstruction is superior to the multichannel MEMSYS result, and is free of the low-level spurious sources and signal-correlated residuals evident in the MEMSYS reconstruction.

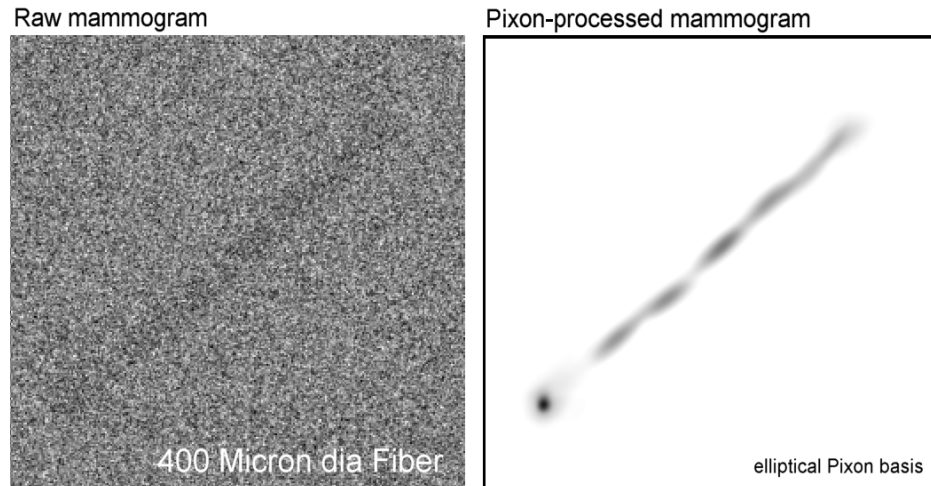
Mammogram (standard phantom, American College of Radiology)

Figure 3. Pixon reconstruction of X-ray mammography data.

4.2. IRAS Imaging of M51

In Fig. 2 we present comparisons of reconstructed images from $60\mu m$ IRAS scans of the interacting galaxy pair M51. This data set was used in an image reconstruction contest at the 1990 MaxEnt Workshop (Bontekoe 1991). As can be seen, the Lucy-Richardson and maximum-correlation (also known as HIRES) reconstructions fail to reduce image spread in the cross-scan direction, i.e., the rectangular signature of the 1.5×4.75 detectors is still clearly evident. They also do not reconstruct even gross features such as the “hole” (black region) in the emission north of the nucleus—this hole is clearly evident in optical images of M51. The MEMSYS 3 reconstruction is significantly better, recovers the hole, and resolves the NE and SW arms of the galaxy into discrete sources. However, the Pixon result is clearly superior. In fact, its sensitivity is a factor of 200 higher than that of MEMSYS 3, and its linear spatial resolution is improved by a factor of 3. The reality of its minute details can be verified by comparing with images at other wavelengths.

4.3. X-Ray Mammography

Presented in Fig. 3 is a Pixon reconstruction of a standard phantom from the American College of Radiology. Here a fiber with a 400 micron diameter was embedded in a piece of material with X-ray absorption properties similar to the human breast. This particular example was selected since it has a low SNR. A family of elliptical Pixon kernel functions was used for the reconstruction. The Pixon method easily detects the presence of the fiber. In some locations, however, the SNR of the fiber is so poor that statistically significant signal is absent. Hence, no detection can be made by the Pixon method.

Acknowledgments. This work was supported in part by NASA grants NAG53944 (to RCP) and AR-07551.01-96A (to AY).

References

- Bontekoe, T. R. 1991, in *Maximum Entropy and Bayesian Methods*, ed. W. T. Grady Jr. & L. H. Schick (Dordrecht: Kluwer), 319
- Bontekoe, T. R., Kester, D. J. M., Price, S. D., de Jonge, A. R. W., & Wesselieus, P. R. 1991, *A&A*, 248, 328
- Burch, S. F., Gull, S. F., & Skilling, J. 1983, *Comp. Vis., Graphics, & Im. Process.*, 23, 113
- Chaitin, G. J. 1966, *J. Ass. Comput. Mach.*, 13, 547
- Donoho, D. L. 1995, *IEEE Trans. Inf. Theory*, 41, 613
- Donoho, D. L. & Johnstone, I. M. 1994, *Comptes Rendus de L'Academie Des Sciences Serie I-Mathematique*, 319, 1317
- Gull, S. F. 1989, in *Maximum Entropy and Bayesian Methods*, ed. J. Skilling, (Dordrecht: Kluwer), 53
- Gull, S. F. & Skilling, J. 1991, *MemSys5 Quantified Maximum Entropy User's Manual*, (Royston: Maximum Entropy Data Consultants Ltd.)
- Kolmogorov, A. N. 1965, *Inf. Transmission*, 1, 3
- Piña, R. K. & Puetter, R. C. 1993, *PASP*, 105, 630
- Press, W. H., Teukolsky, S. A., Vetterling, W. Y., & Flannery, B. P. 1992, *Numerical Recipes in Fortran (2nd ed.)*, (Cambridge: Cambridge Univ. Press)
- Puetter, R. C. 1994, in *SPIE Proc.*, Vol. 2302, *Image Reconstruction and Restoration*, ed. T. J. Schulz & D. L. Snyder, (Bellingham: SPIE), 112
- , 1995, *Int. J. Image Sys. & Tech.*, 6, 314
- , 1997, in *Instrumentation for Large Telescopes*, ed. J. M. Rodriguez Espinosa, A. Herrero, & F. Sanchez, (Cambridge: Cambridge Univ. Press), 75
- Puetter, R. C. & Piña, R. K. 1993, in *SPIE Proc.*, Vol. 1946, *Infrared Detectors and Instrumentation*, ed. A. M. Fowler, (Bellingham: SPIE), 405
- , 1994, in *Science with High Spatial Resolution Far-Infrared Data*, (JPL Publ. 95-4), (Pasadena: JPL), 61
- Rice, W. 1993, *AJ*, 105, 67
- Shannon, C. E. 1948, in *Key Papers in the Development of Information Theory*, ed. D. Slepian, (New York: IEEE Press), 1974
- Skilling, J. 1989, in *Maximum Entropy and Bayesian Methods*, ed. J. Skilling, (Dordrecht: Kluwer), 45
- Solomonoff, R. 1964, *Inf. Control*, 7, 1
- Weir, N. 1991, in *Proc. of the ESO/ST-ECF Data Analysis Workshop*, ed. P. Grosbo & R. H. Warmels, (Garching: ESO), 115
- Wiener, N. 1949, *Extrapolation and Smoothing of Stationary Time Series*, (New York: Wiley)